

Article

Relationship among Electrical Signals, Chlorophyll Fluorescence, and Root Vitality of Strawberry Seedlings under Drought Stress

Juan Zhou ^{1,†}, Weidong Yuan ^{2,†}, Bao Di ² , Guanghua Zhang ², Jianxi Zhu ³, Pengyu Zhou ², Tianran Ding ⁴ and Ji Qian ^{2,*} 

- ¹ College of Mechatronics & Electrical Engineering, Hebei Agriculture University, No. 289 Lingyusi Street, Baoding 071001, China; jdzj@hebau.edu.cn
- ² College of Horticulture, Hebei Agriculture University, Lekai South Street 2596, Baoding 071000, China; ywd9924@163.com (W.Y.); dibao666@126.com (B.D.); yyzgh@hebau.edu.cn (G.Z.); 13303308759@163.com (P.Z.)
- ³ Zhejiang Agricultural Machinery Research Institute, 1158 Zhihe Rd, Jinhua 321051, China; zhujianxi829@163.com
- ⁴ Institute for Environmental Management and Land-Use Planning, Université Libre de Bruxelles (ULB), Av. FD. Roosevelt 50, 1050 Brussels, Belgium; tianran.ding@outlook.com
- * Correspondence: yyqj@hebau.edu.cn or qianji167@163.com; Tel.: +86-312-7528304
- † These authors contributed equally to this work.

Abstract: Drought area expansion has a great impact on the growth and development of plants. To contribute to the water management of strawberry, this work aims to study the chronological relationship between the electrical signals and representative physiological parameters of strawberry seedlings under drought stress. This study analyzed the characteristic variables of the electrical signals; physiological parameters under drought; and control treatments. Moreover, we compared the chronological sequence of the appearance of significant differences between drought and control treatment in terms of their physiological parameters and electrical signals. The results showed that with the increase of drought treatment, the time domain parameters (peak-to-peak value, standard deviation) and frequency domain parameters (spectral of central gravity, power spectrum entropy) of the drought-treated electrical signals showed significant differences from the control on Day 2 and Day 6, respectively ($p < 0.05$). The root vitality of the drought treatment was significantly different from the control on Day 4 ($p < 0.05$); the F_v/F_m and the $SPAD$ were significantly different ($p < 0.05$) on Day 7. Electrical signals first start to show a significant difference between drought and control treatment, followed by physiological parameters. Therefore, the electrical signal can be used as an early indicator of drought stress conditions. This will provide a scientific basis for the actual water management of strawberry seedlings. It also provides a methodological and theoretical basis for other studies analyzing the relationship between plant physiological parameters and electrical signals under other stress conditions.

Keywords: strawberry; drought stress; electrical signals; physiological parameters



Citation: Zhou, J.; Yuan, W.; Di, B.; Zhang, G.; Zhu, J.; Zhou, P.; Ding, T.; Qian, J. Relationship among Electrical Signals, Chlorophyll Fluorescence, and Root Vitality of Strawberry Seedlings under Drought Stress. *Agronomy* **2022**, *12*, 1428. <https://doi.org/10.3390/agronomy12061428>

Academic Editor: Alfonso Albacete

Received: 28 May 2022

Accepted: 13 June 2022

Published: 14 June 2022

Publisher's Note: MDPI stays neutral with regard to jurisdictional claims in published maps and institutional affiliations.



Copyright: © 2022 by the authors. Licensee MDPI, Basel, Switzerland. This article is an open access article distributed under the terms and conditions of the Creative Commons Attribution (CC BY) license (<https://creativecommons.org/licenses/by/4.0/>).

1. Introduction

According to the Intergovernmental Panel on Climate Change (IPCC), drought events have become the most severe natural disaster in many regions of the world [1]. With the expansion of global arid and semi-arid areas, water scarcity has become one of the most critical ecological problems in the 21st century [2–4], and soil drought has become one of the most common and harmful environmental stresses [5]. Drought is an environmental state that disrupts the water balance of plants and has a dehydrating effect on them [6]. Under drought stress, various aspects of plants are changed to varying degrees, including apparent morphology (e.g., leaf color, leaf shape), internal tissue structure (e.g., the membrane system of cells), molecules (e.g., expression of resistance genes), and electrical

signals (e.g., conduction rate, membrane transport, and electrostatic potential distributions). Furthermore, researchers have found that drought stress inhibits plants' growth rate and status, even leading to death [7].

As one of the fruit crops with high economic value and wide cultivation globally, strawberries are important for agricultural development. However, strawberries are sensitive to drought stress due to their fast growth rate and shallow root distribution, requiring a large amount of water for transpiration. Strawberries are water-demanding but have a low tolerance for waterlogging. These characteristics make the drought stress and its effect on the internal water deficiency the first among all abiotic factors for strawberry growth [8]. Therefore, studying the effects of drought stress on strawberries is meaningful for their water management [9].

In the research on the effects of stress on plants, physiological parameters are used as important parameters in many experiments. For example, Krzysztof Klamkowski and Waldemar Treder [10] studied the response of three strawberry varieties ('Elsanta', 'Elkat', and 'Salut') to drought stress in terms of morphological and physiological parameters. They found that 'Elsanta' was the most drought-tolerant. Nasser Ghaderi and Adell Siosemardeh [11] found that different levels of drought stress affect different physiological parameters of strawberry seedlings. Their results showed that moderate drought stress affects gas exchange and severe drought stress affects chlorophyll, proline, and soluble carbohydrate. Xue Xinping et al. [12] found that apple root vitality showed a trend of increasing and then decreasing under drought stress. Xiao Shihong et al. [13] found that chlorophyll content of *Heritiera littoralis* seedlings showed a pattern of increasing and then decreasing as drought stress intensifies. Yiji Shi [14] found that under drought stress, several physiological parameters of the *Sassafras tsumu* seedling present a pattern of increasing and then decreasing, including leaves superoxide dismutase (SOD) activity, peroxidase (POD) activity, soluble sugar, soluble protein, proline, and chlorophyll. Zhang et al. [15] studied the effect of drought stress on the chlorophyll content of five strawberry varieties at the seedling stage. Their results showed significant differences in chlorophyll in different strawberry varieties.

In addition to the study of physiological parameters, the effect of external stress on electrical signals has also attracted researchers' attention. Electrical signals in plants were first discovered in *Dionaea muscipula* by Sanderson [16] in 1873 and are considered a widespread phenomenon in the plant kingdom. Electrical signals are weak, low-frequency, unstable signals transmitting between cells and tissues. They are involved in many plants' life processes, including respiration, water uptake, leaf movement, and biotic stress responses. Researchers have found that the electrical signals produced by plants may be related to the plant response to adversity stress. For example, plants produce significant action potentials after mechanical damage or insect attack [17]. Studies by Schroeder and Hedrich [18] showed that plant osmosis affects electrical signal production from the perspective of ion. In addition, the type and strength of electrical signals are related to the type and intensity of the stimulus [19]. For example, Datta and Palit [20], Chatterjee et al. [21], and Wang et al. [22] studied the changes in plant electrical signals under different light stimuli. Their results showed that the intensity of plant electrical signals increased with light intensity. Compared to other parameters such as enzymes, hormones, and metabolites, electrical signals could also respond to water stress [23]. Current research has focused on the changes in physiological parameters and plant electrical signals under environmental stress, respectively. As far as we know, no article has been conducted to study the relationship between changes in plant physiological parameters and electrical signals under drought stress.

We studied the changes in physiological parameters and electrical signals of a common annual strawberry—"Tokun"—during drought stress. The aim of this experiment was to study the effects of drought stress on physiological parameters and electrical signal production in strawberry seedlings, especially their chronological sequence regarding the appearance of significant differences compared to their associated control treatment. The results can provide a theoretical basis and rationale for the study of strawberry water management.

2. Materials and Methods

2.1. Experiment Design

This experiment was carried out in the greenhouse environment of Hebei Agricultural University Teaching Experiment Base (115°29'24" E, 38°51'21" N), Baoding City, Hebei Province. We covered the roof of the open greenhouse (dimensions 6 m × 40 m) with plastic sheeting to avoid rainwater but left four sides open to enhance air circulation during the experiment.

The material for this experiment was strawberry “Tokun” stolon seedlings of the current year. ‘Tokun’ was developed from a cross between synthetic decaploids K58N7-21 (‘Karen berry’ × *Fragaria nilgerrensis*) as the seed parent and ‘Kurume IH No. 1’ (‘Toyonoka’ × *F. nilgerrensis*) as the pollen parent at the NIVTS, Japan. We selected strawberry seedlings with 4–5 leaves and 20–30 cm in height. On 1 September 2020, we established them in the plastic pots containing a seedling soil matrix (perlite, peat soil, and vermiculite in a 1:1:1 mix by mass, pH = 6.0). Each pot has a round hole in the bottom. They are 18.5 cm in top diameter, 22 cm in height, and 12.5 cm in bottom diameter. Until 12 June 2021, the seedlings were kept in the pots. We measured the water content of the soil in all pots and maintained the values at 75% to 85% of the maximum field water capacity.

The experiment lasted eight days, from 13 June 2021 (Day 1) to 20 June 2021 (Day 8). There are two treatments: drought treatment (DR) and control treatment (CTRL). In the DR treatment, seedlings were watered slowly at 21:00 on June 12 (one day before the experiment started) until water seeped out of the bottom of the pot. Throughout the experiment (Day 1–Day 8), seedlings in the DR will not be watered. In contrast, seedlings in CTRL treatment were watered at 21:00 every day to keep the relative soil water content in the pots at about 70% of the maximum field water capacity. The volumetric soil water content was measured by a soil moisture meter (TDR100, Spectrum Technologies, Inc., Plainfield, IL, USA) at 9:00, 15:00, and 22:00 each day (Figure 1).

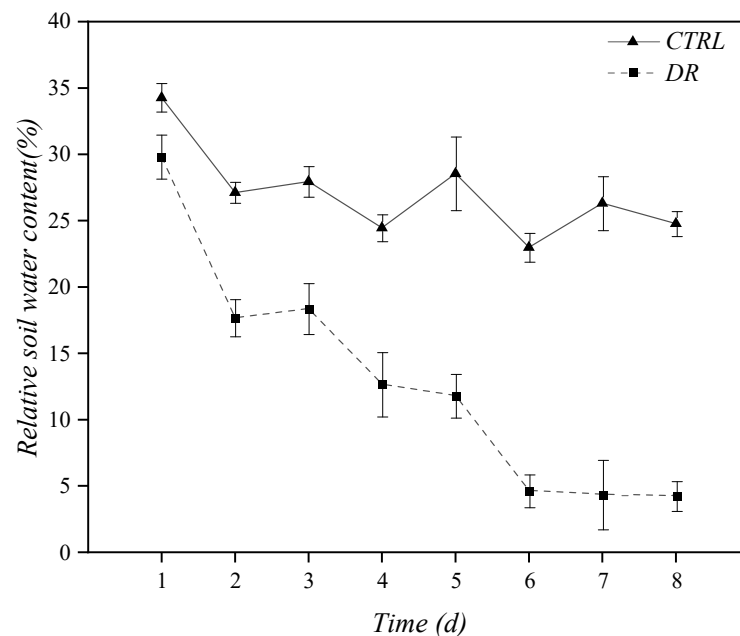


Figure 1. The change in the relative water content of the soil during the experiment period (Day 1–Day 8), i.e., control (CTRL), drought (DR).

We measured these parameters three times per day (9:00 to 9:40, 15:00 to 15:40, and 20:00 to 20:40) for eight consecutive days (in total 24 times) to make the results more intuitive and accurate. On Day 1, one pot was randomly selected from each treatment (a total of 2 pots for two treatments) for in situ measurements of the electrical signal parameter. The physiological parameters were measured in five replicates for each treat-

ment, and three pots of strawberry seedlings were randomly selected for each replicate; 240 (2 treatments \times 5 replicates \times 3 strawberry seedlings \times 8 times sampling = 240) pots of the test material were required, and 242 (240 for physiological parameters and 2 for electrical signal measurement) pots of experimental material were required for the whole experiment.

2.2. Indicator Measurement and Method

2.2.1. Electrical Signals' Measurement and Treatment

The electrical signals were first collected (Collecting Electrical Signals Section), followed by signal treatment, including reducing frequency (Reducing Frequency of Electrical Signal Section) and denoising (Denoising for Electrical Signal Section). The treated electrical signals were analyzed from time-domain and frequency-domain perspectives (Section 3.1). The former (time-domain analysis) includes three parameters: peak-to-peak value (PTP), mean value (mean), and standard deviation (SD), while the latter (frequency-domain analysis) includes two parameters: the Spectral of Central Gravity (SCG) and power spectrum entropy (PSE).

Collecting Electrical Signals

We first collected electrical signals from plants using the BL-420N biological signal acquisition and analysis system, designed and produced by Chengdu Taimeng Software Co., Ltd. Two electrodes were inserted into the strawberry stem to a depth of 2 mm, the positive electrode was inserted 100 mm from base, and the negative electrode was inserted 180 mm from the base, with an interval of 80 mm between them; the ground wire was connected to the base of the strawberry rhizomes. The strawberry samples and BL-420N instrument were placed into a 200-mesh 50 cm \times 50 cm copper faraday cage to shield noise signals in the external environment (Figure 2). Electrical signals were formally collected 30 min after the electrodes were inserted to eliminate the polarization of the electrodes. We collected 0.6 million data for 10 min.

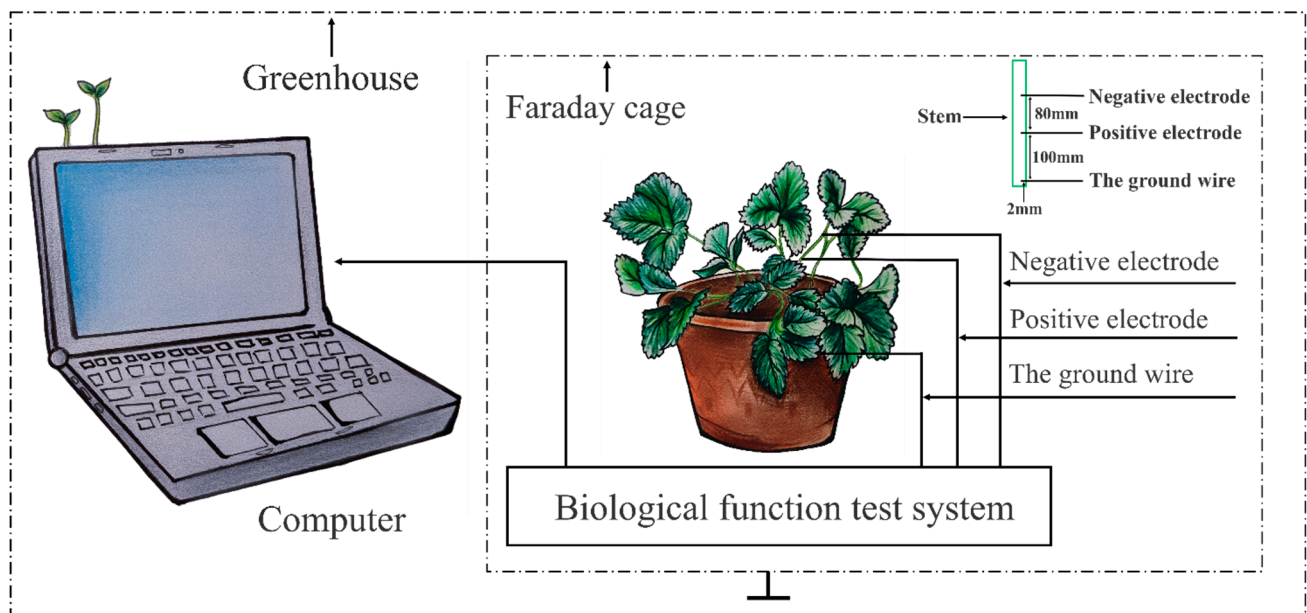


Figure 2. A schematic diagram of the electrical signal collection device and its location. The strawberry seedlings were connected to the electrical signal collection device with conduction electrodes within the Faraday cage (denoted with dashed line). The computer was connected to the collection device with a data acquisition cable. The strawberry seedlings and the electrical signal acquisition device were placed in a Faraday cage, while the computer was placed outside the Faraday cage. The whole process was carried out in the greenhouse.

BL-420N parameters were set as follows. No external excitation signal was added; the range was 500 μV ; the sampling frequency was 1 kHz; and a 50 Hz notch filter was set to open to filter out the interference of power frequency signal interference. As the frequency of plant electrical signals is generally less than 10 Hz [24], bandpass filtering was carried out for them, and the low-pass cut-off frequency was set as 20 Hz. The high-pass cut-off frequency is determined by Equation (1),

$$f_H = \frac{1}{2\pi T} \quad (1)$$

where the time constant T is selected as 5 s in the instrument option, so the high-pass cut-off frequency f_H is 0.032 Hz.

Reducing Frequency of Electrical Signal

The frequency of the plant electrical signal without external excitation is generally less than 10 Hz. According to the Nyquist–Shannon sampling theorem:

$$f_s \geq 2f_m \quad (2)$$

where f_m is the maximum frequency component of the signal and f_s is the Nyquist frequency. We assign $f_m = 10$ Hz, then $f_s \geq 40$ Hz. Generally, 2 to 3 times this value is selected, and the frequency of the collected electrical signal of strawberry seedlings is reduced by selecting $f_s = 50$ Hz.

Denosing for Electrical Signal

The signal of strawberry seedlings will inevitably be mixed with White Gaussian Noise generated by the measuring instrument. To effectively remove the white Gaussian noise mixed into the electrical signal, this experiment adopted the Wavelet Threshold Denoising Method to denoise the collected electrical signal [25].

The effect of wavelet threshold denoising is affected by different wavelet basis functions, decomposition levels, threshold selection rules, and thresholding functions. In this experiment, the db5 wavelet basis function (dbN) was selected to carry out 5-level decomposition, and the minimax criterion was selected as the determination method of the threshold. Equation (3) presents the threshold function.

$$Th = \begin{cases} 0, N \leq 32 \\ \sigma(0.3936 + 0.1829 \log_2 N), N > 32 \end{cases} \quad (3)$$

where $\sigma = \text{median}(\frac{|\omega|}{0.6745})$, ω is the wavelet coefficient vector at unit scale, and N is the length of the signal vector [26].

According to the threshold determined by Equation (3), the soft thresholding function of Equation (4) was applied to filter the decomposed wavelet coefficients. When the wavelet coefficients $|\omega|$ are greater than the given threshold, the difference between the wavelet coefficients $|\omega|$ and the threshold Th is multiplied by the sign function $\text{sgn}(\omega)$ as the modified wavelet coefficients [27]. Finally, the waveforms of each component after filtering are reconstructed to the filtered strawberry electrical signal. The soft threshold function is

$$\omega_{Th} = \begin{cases} [\text{sgn}(\omega)](|\omega| - Th) & |\omega| \geq Th \\ 0 & |\omega| < Th \end{cases} \quad (4)$$

2.2.2. Physiological Parameters

This experience measured three physiological parameters: root vitality, maximal photochemical efficiency, and relative chlorophyll content.

Root Vitality (RV)

This study measured root vitality with TTC (2,3,5-Triphenyltetrazolium chloride) method [28]. New root tips (0.3 g) were taken from each sample and placed in a beaker, followed by 0.4% TTC solution, 0.1 mol/L phosphoric acid buffer (pH = 7.0), and 2 mL of 1 mol/L sulfuric acid. Subsequently, ethyl acetate and quartz sand were added and grinded. Finally, ethyl acetate was added to the grinded solution, of which the absorbance value at 485 nm was determined. According to the standard curve, the reduction amount of TTC was determined. Based on Equation (5), we calculate the RV.

$$TTC = \frac{TTC \text{ reduction volume}(g)}{Root \text{ weight}(g) \times Time(h)} \quad (5)$$

Maximal Photochemical Efficiency (F_v/F_m)

One leaf was randomly selected from the middle part of the plant in each pot and fixed directly with a dark processing clip. The samples' minimal fluorescence value (F_0) and maximal fluorescence value (F_m , the maximum value after excitation by 0.8 s 3000 mmol·m⁻²·s⁻¹ saturating pulse of light) were measured with a portable fluorescence analyzer (HandyPEA, Hansatech, UK) after dark adaptation for 20 min. Measurements were made in situ, and the veins were avoided. The maximum photochemical efficiency of photosystem II was determined by F_v/F_m (F_v is variable fluorescence) ratio, where $F_v = F_m - F_0$.

The Relative Amount of Chlorophyll (SPAD Value)

The relative chlorophyll content was measured using a handheld SPAD (soil plant analysis development) instrument (SPAD-502Plus, KONICA MINOLTA), which we refer to as the SPAD value. Nine clean leaves were randomly selected from each plant's middle and upper parts for in-situ measurement (three leaves in each upper, middle, and lower parts). The veins of the plants were avoided in the measurement.

2.2.3. Data Treatment and Analysis

Matlab software (2018, The MathWorks Inc., Natick, MA, USA) was used to perform frequency reduction and denoising and calculate time-domain parameters (PTP, mean, SD) and frequency domain parameters (SCG, PSE) for the collected electrical signal data.

We used the indirect method of power spectrum estimation, also known as the Blackman–Tukey (BT) method [29], the theoretical basis of which is the Wiener–Khinchine theorem. The specific steps are presented below. First, we define $x_N(n)$ the sample sequence of the signal, which was used to calculate the autocorrelation function $R_{xx}(m)$. Then, the Fourier transform of the autocorrelation function $R_{xx}(m)$ was obtained. Finally, the power spectrum estimation $P(k)$ of $x_N(n)$ was obtained. Its mathematical expression is

$$P(k) = \sum_{m=-M}^M R_{xx}(m) W_N^{-mk} \quad (6)$$

SCG indicates the distribution of gravity center of signal power according to frequency. Its value was calculated based on Equation (7):

$$f_g = \frac{\sum_{f=f_1}^{f_2} [P(f) \times f]}{\sum_{f=f_1}^{f_2} p(f)} \quad (7)$$

where f_g is SCF, $f_1 \sim f_2$ is the frequency range, $P(f)$ is the signal's power, and f is the frequency value.

PSE reflects the complexity of the signal, as defined in Equation (8)

$$H_f = -\sum p_f \ln p_f \quad (8)$$

where the subscripts f is the frequency and p_f is the percentage of the power at the frequency f in the whole power spectrum.

Finally, we analyzed the results for five electrical signal parameters (PTP, mean, SD, SCG, and PSE) and four physiological parameters (RV, F_v/F_m , and SPAD) using a mixed linear model (procedure MIXED in IBM SPSS Statistics 22.0, IBM Co., New York, NY, USA). The model is

$$y = \mu + treatment + time + treatment \times time + \varepsilon \quad (9)$$

where μ is mean overall treatment and time, treatment (i.e., DR and CTRL), and time (i.e., the sampling time) are fixed factors, and residual ε represents random terms. The significance of the difference between the treatments at different sampling times was tested by contrasts using Bonferroni-corrected significance levels.

3. Results

3.1. Electrical Signal

3.1.1. Time-Domain Analysis

The electrical signals of strawberry seedlings are roughly distributed between $-600 \mu\text{V}$ and $150 \mu\text{V}$. There is no definite change pattern, reflecting its random and weak characteristics (Figure 3). On Day 1, for CTRL treatment, the electrical signal values in the morning and afternoon were distributed from $-100 \sim 100 \mu\text{V}$. There was an obvious spike pulse appeared (-210 V) in the afternoon measurement. The electrical signal values in the evening were distributed from $-150 \sim 100 \mu\text{V}$. For DR treatment, most of the electrical signal values in the morning were from $-50 \sim 50 \mu\text{V}$, but there were several spike pulses with values up to about $-120 \mu\text{V}$. Most of the electrical signal values in the afternoon were distributed from $-50 \sim 50 \mu\text{V}$. The electrical signal values at night were distributed from $-50 \sim 50 \mu\text{V}$, and there were also several spikes, with the maximum value reaching $-250 \mu\text{V}$.

On Day 2, the electrical signal measured in the morning, afternoon, and evening were distributed from $-100 \sim 150 \mu\text{V}$, $-50 \sim 50 \mu\text{V}$, and $50 \sim 50 \mu\text{V}$, respectively, in the CTRL treatment. For DR treatment, electrical signals measured in the morning were mostly distributed from $-100 \sim 100 \mu\text{V}$, but they changed more drastically since there were many spike pulses, the maximum value of which was close to $-600 \mu\text{V}$. Most of the electrical signal values were distributed from $-100 \sim 100 \mu\text{V}$, and $-75 \sim 100 \mu\text{V}$ in the afternoon and the evening, respectively.

During the drought stress period, the time-domain parameters of the electrical signal of strawberry seedlings were analyzed (Figure 4, Table 1). The results show that the PTP of the control group present an overall pattern of a decrease followed by an increase. The PTP tend to be around $230 \mu\text{V}$ from Day 5 to Day 8.

The PTP in the DR treatment has a significant difference from the CTRL treatment, i.e., first increasing followed by decreasing and reaching a maximum value of $345.96 \mu\text{V}$ on Day 2. The ranges of the mean in the CTRL and the DR were $-0.5 \mu\text{V}$ to $1.4 \mu\text{V}$, and $-0.5 \mu\text{V}$ to $0.80 \mu\text{V}$, respectively. Their trends were the same, and no significant differences were observed throughout the stress period. The SD in the CTRL treatment showed an overall trend of decreasing and then increasing, which is opposite to DR treatment (increasing and then decreasing, reaching a maximum value of $41.60 \mu\text{V}$). There was a significant difference between DR and CTRL treatment on Day 2 at the 0.005 level (98.76% higher than the CTRL treatment). Moreover, Day 3, Day 5, and Day 6 also showed significant differences between DR and CTRL treatment ($p < 0.05$).

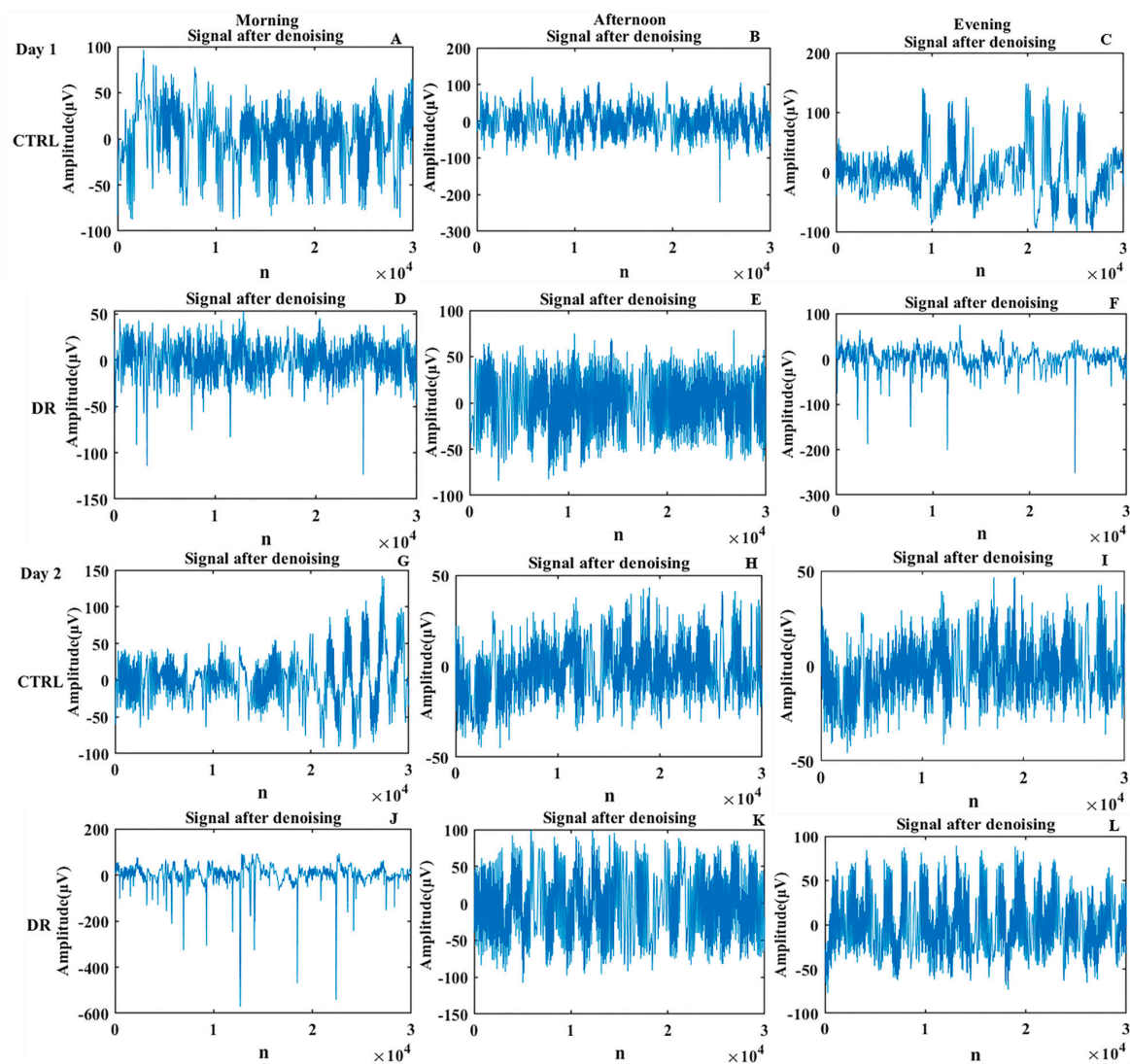


Figure 3. The denoising results on Day 1 and Day 2. Graphs (A–C) correspond to the results of the control treatment measured in the morning, afternoon, and evening on Day 1; (D–F) correspond to the results of the drought treatment measured in the morning, afternoon, and evening on Day 1. (G–I) correspond to the results of the control treatment measured in the morning, afternoon, and evening on Day 2; (J–L) correspond to the results of the drought treatment measured in the morning, afternoon, and evening on Day 2.

Table 1. The statistics of significant differences of each parameter between the drought treatment and the control treatment during the experiment (Day 1–Day 8).

Pairwise Comparison	Process-Time							
	1 d	2 d	3 d	4 d	5 d	6 d	7 d	8 d
PTP	0.875	0.012 *	0.324	0.339	0.150	0.105	0.456	0.255
Mean	0.694	0.314	0.267	0.674	0.450	0.578	0.421	0.624
SD	0.131	0.005 **	0.047 *	0.130	0.025 *	0.015 *	0.319	0.066
SCG	0.245	0.940	0.793	0.600	0.079	0.010 *	0.063	0.172
PSE	0.255	0.530	0.132	0.375	0.521	0.002 **	0.206	0.535
RV	0.394	0.700	/	0.010 *	/	/	0.006 **	0.027 *
Fv/Fm	0.611	0.939	0.598	0.768	0.596	0.618	0.006 **	0.000 **
SPAD	0.253	0.956	0.313	0.585	0.529	0.678	0.048 *	0.042 *

* The difference is significant at the 0.05 level; ** the difference is significant at the 0.01 level.

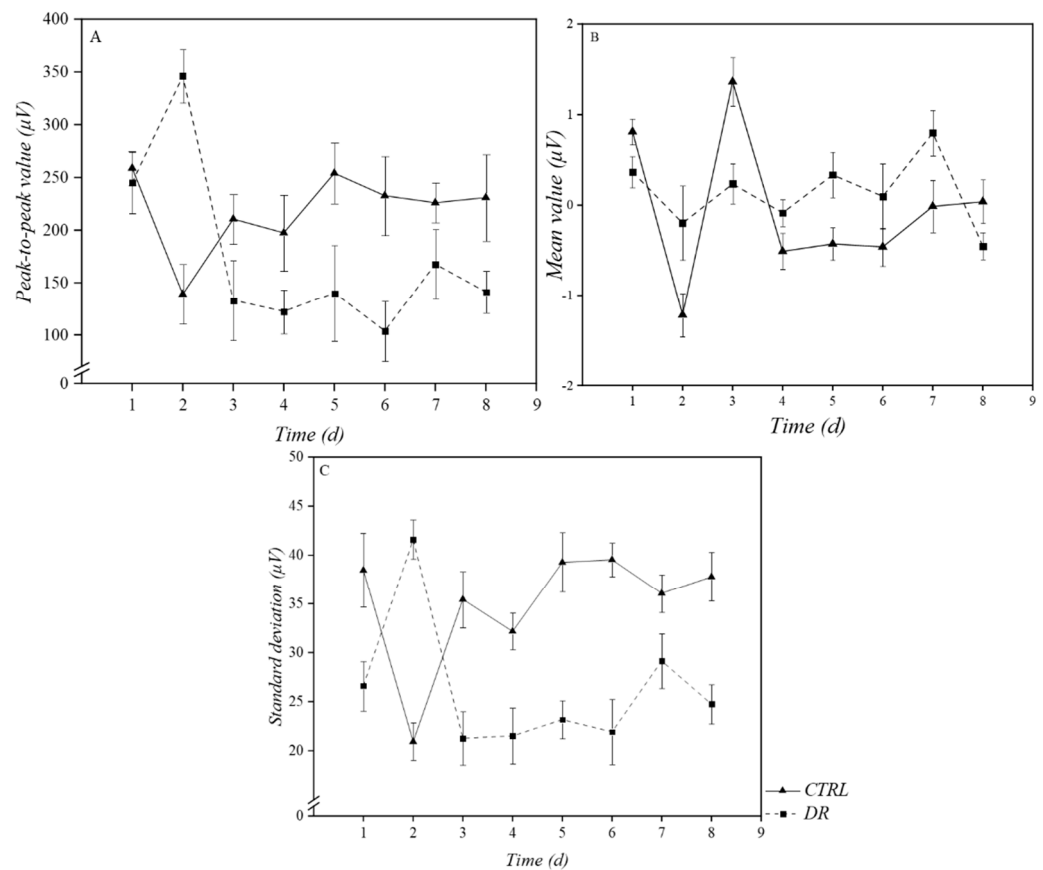


Figure 4. The change of time-domain parameters during the experiment (Day 1–Day 8). (A) is the change of peak-to-peak value; (B) is the change of mean value; and (C) is the change of standard deviation; i.e., control (CTRL), drought (DR).

3.1.2. Frequency-Domain Analysis

The signal frequencies for both CTRL and DR treatment were concentrated below 5 Hz (Figure 5). Therefore, any small signal above 5 Hz was considered noise. The amplitude of the electrical signal was larger when it was less than 2 Hz. It quickly decayed when it was larger than 2 Hz, which shows that the power spectral estimation was mainly concentrated in the low-frequency range. Above 3 Hz, most of the frequency components amplitude were attenuated to below -10 dB/Hz, and most noise signals were filtered out.

On Day 1, the maximum amplitudes of the frequency component in the CTRL treatment were all close to 35 dB/Hz for all three periods of measurement. For the DR treatment, the maximum amplitude was close to 35 dB/Hz in the evening and 30 dB/Hz in the morning and afternoon. A denser spectral was found from -10 dB/Hz~ -20 dB/Hz in the afternoon.

On Day 6, the maximum frequency component amplitude in CTRL and DR treatments in three measurement periods were close to 40 dB/Hz and 30 dB/Hz, respectively. In the afternoon, a denser spectral (from -10 dB/Hz~ -20 dB/Hz) was found for the CTRL and DR treatments.

During the drought stress, while the SCG in the CTRL treatment presents an overall trend of increasing and decreasing, the values in the DR treatment showed a trend of increasing, then decreasing, and then increasing, reaching a minimum value of 0.28 Hz on Day 3 (Figure 6, Table 1). There was a significant difference between DR and CTRL treatments on Day 6 ($p = 0.010$, 131.58% higher than the CTRL). The PSE in the CTRL treatment showed an overall trend of decreasing and then increasing. The PSE of the DR treatment reached a maximum value of 5.86 on Day 6, showing a highly significant difference with the CTRL ($p = 0.002$), and was 33.33% higher than that of the control.

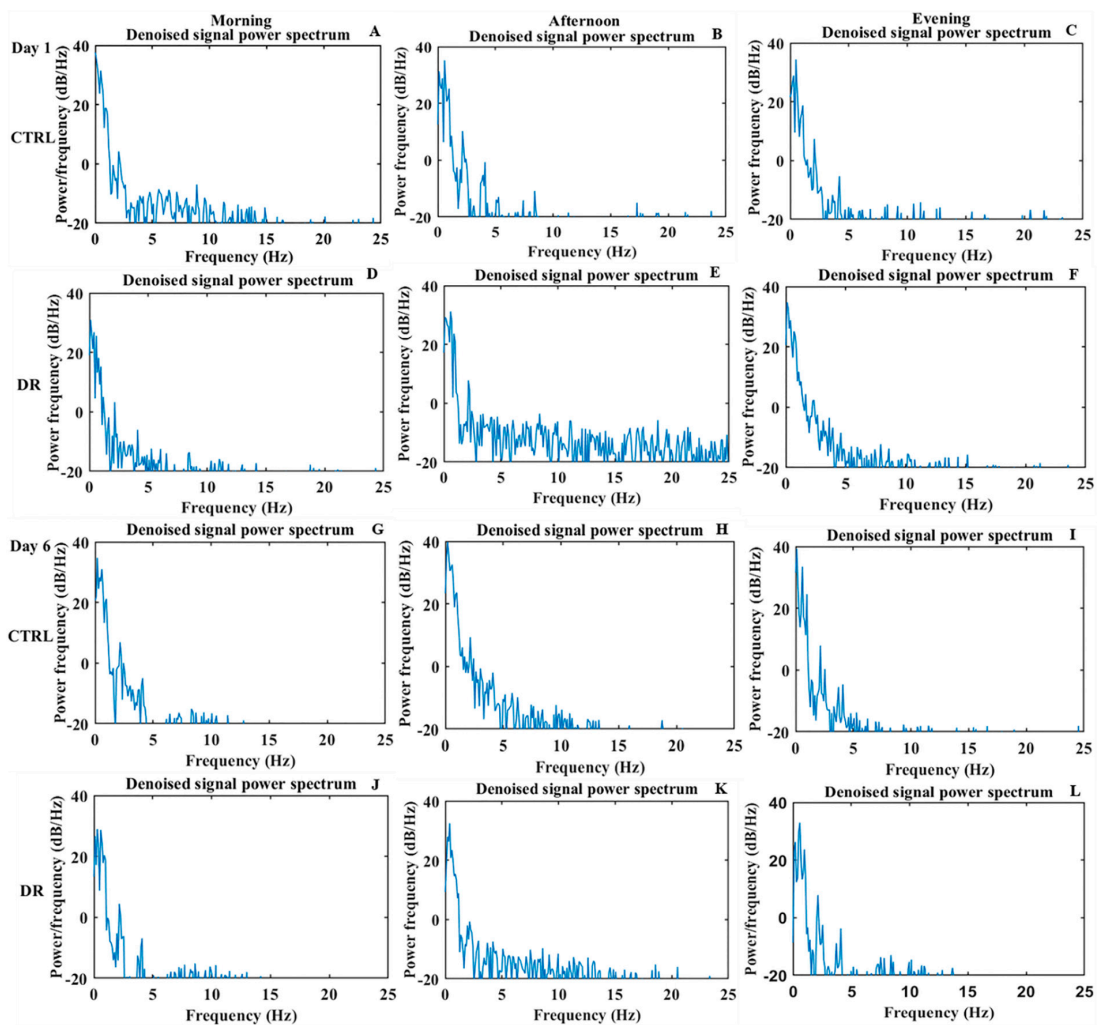


Figure 5. The power spectrum of denoised signals on Day 1 and Day 6. Graphs (A–C) correspond to the results of the control treatment measured in the morning, afternoon, and evening on Day 1; (D–F) correspond to the results of the drought treatment measured in the morning, afternoon, and evening on Day 1; (G–I) correspond to the results of the control treatment measured in the morning, afternoon, and evening on Day 6; and (J–L) correspond to the results of the drought treatment measured in the morning, afternoon, and evening on Day 6.

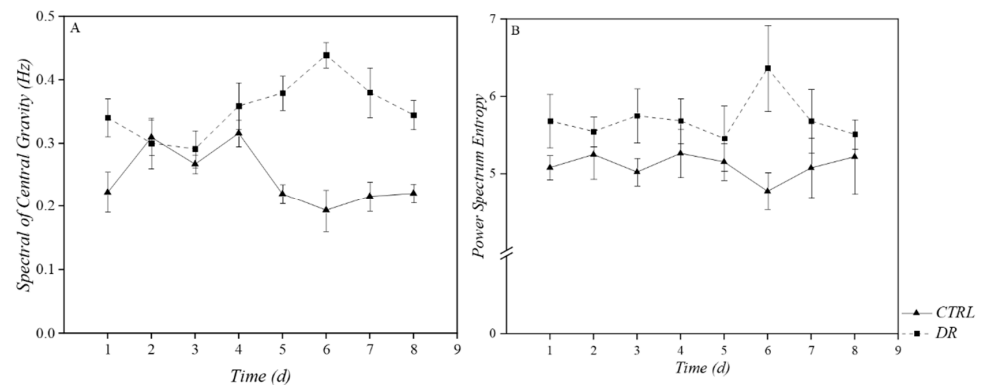


Figure 6. The change of time-domain parameter during the experiment (Day 1–Day 8). (A) is the change of Spectral of Central Gravity; (B) is the change of power spectrum entropy; i.e., control (CTRL), drought (DR).

3.2. Physiological Indicator Results

During drought stress, the RV values in the CTRL and DR treatment generally tended to increase and then decrease, with the value in the DR treatment reaching a maximum value of 0.07 on Day 4 and being significantly ($p = 0.010$) lower than that in the CTRL (41.67%) (Figure 7A, Table 1). The RV value in the DR treatment reached a minimum value of 0.01 on Day 8 and was significantly ($p = 0.027$) lower than that of the CTRL (83.33%).

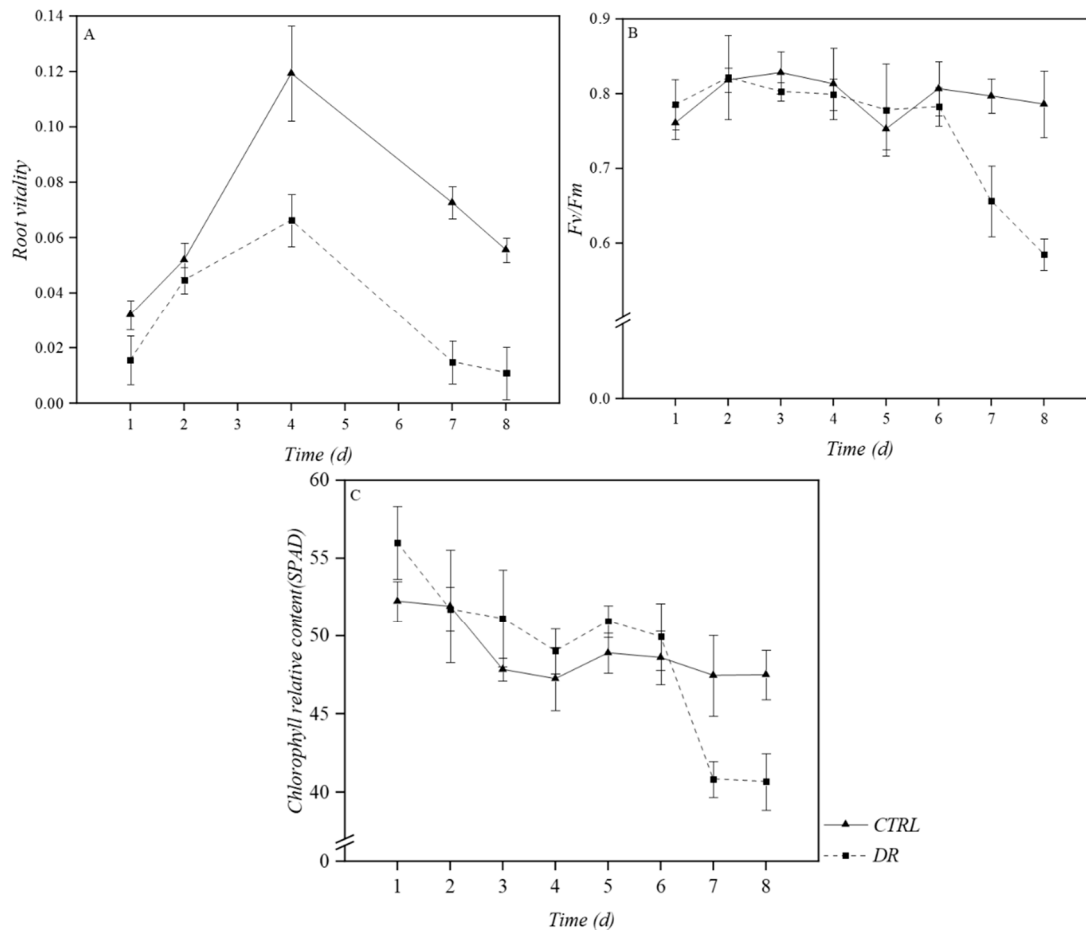


Figure 7. The change of physiological parameters during the experiment (Day 1–Day 8). (A) is the change of root vitality, (B) is the change of F_v/F_m , (C) is the change curve of SPAD values; i.e., control (CTRL), drought (DR).

During drought stress, the F_v/F_m in the DR treatment generally tended to increase and then decrease, reaching a maximum value of 0.82 on Day 2, 0.45% higher than the control (Figure 7B, Table 1). The maximum photochemical efficiency value in the DR treatment was significantly ($p = 0.006$) lower than that of the CTRL on Day 7. On Day 8, the values of F_v/F_m in the DR treatment reached the minimum value of 0.59, which is significantly ($p = 0.000$) lower than that of the control (25.56%).

There was an overall decrease in SPAD values in the DR and CTRL treatments (Figure 7C, Table 1). There was no significant difference in their values until Day 7, on which values in the DR treatment were significantly lower ($p = 0.048$) than that of CTRL treatment. On Day 8, the SPAD reached a minimum value of 40.68 and was significantly ($p = 0.042$) lower (14.34%) than the control.

3.3. Chronological Relationship between Electrical Signals and Physiological Parameters

During drought stress, all three physiological parameters measured showed significant differences at different times of stress (Figure 8). Four of the five electrical parameters

measured showed significant differences, with one not showing a significant difference. Collectively, seven parameters showed significant differences. Furthermore, five out of seven showed significant differences before and on Day 6, four of which were electrical parameters and one of which was a physiological parameter. Two parameters showed significant differences on Day 7, which were physiological parameters. Therefore, it could be observed that electrical signals precede physiological signals to reflect plant growth conditions under drought stress.

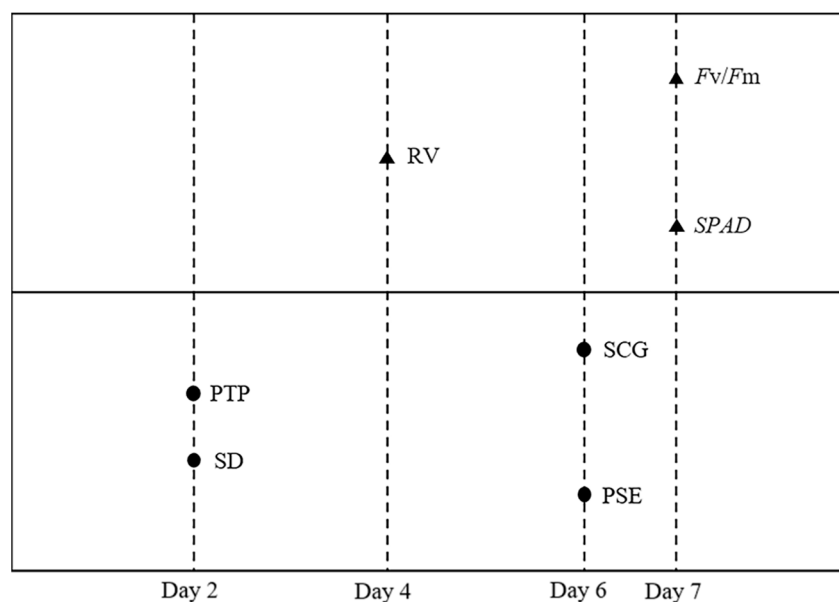


Figure 8. A schematic comparison of electrical signals and physiological parameters that showed significant differences between drought and control treatments (Day 1–Day 8), with triangles indicating physiological parameters and dots indicating electrical parameters. PTP was peak-to-peak value, mean was mean value, SD was standard deviation, SCG was the Spectral of Central Gravity, and PSE was power spectrum entropy. RV was Root Vitality, SPAD was the Relative Amount of Chlorophyll, and F_v/F_m was Maximal Photochemical Efficiency.

4. Discussion

The part of the plant that is most sensitive to stress is the leaf, which directly reflects the plant's ability to adapt to adversity [30]. It has been shown that plant morphology and physiological characteristics are altered when plants are subjected to drought stress [31]. In this experiment, 60% of the results concerning RV measured during drought stress showed significant differences between the CTRL and DR treatments. The RV of the seedlings showed a clear tendency to decrease as the degree of stress increased. This phenomenon is probably because as the water in the root system gradually decreases, the cytosol concentration of the plant cells gradually increases, the free water content decreases, and plant metabolism becomes slower, resulting in a greater change in RV. Drought stress affects the photochemical reactions of the leaves, triggering photoinhibition that will result in more light energy being absorbed by the leaves than the plant can use. Therefore, the excess light energy causes photooxidative stress [32–36].

This experiment found that F_v/F_m did not differ significantly between the DR and CTRL treatment from Day 1 to Day 6. On the next two days (Day 7 and Day 8), F_v/F_m in the DR treatment was significantly lower than the CTRL. These results may indicate that plants activated their physiological defenses from Day 1 to Day 6 to reduce the damage caused by external conditions, leaving F_v/F_m in a more stable state. In contrast, from Day 7, the photosynthetic mechanism of the leaves may be damaged to a certain extent as the stresses intensify. Specifically, the chlorophyll may be degraded, hindering photosynthetic electron transmission and decreasing plants' photosynthetic rate. Chlorophyll is the main pigment

for photosynthesis in plants, which gradually increases as the plants grow under normal conditions [37]. Under drought stress, the amount of chlorophyll content in the plant affects the light energy conversion rate of the plant and the formation of photosynthetic products in the plant. Our results proved this explanation. We found that the *SPAD* (Chlorophyll) values in the DR treatment showed less significant changes during the beginning of the drought stress. However, as the stress became more severe, *SPAD* values in the DR treatment decreased significantly compared to the CTRL treatment. Therefore, as the degree of stress increases, the chlorophyll content in the plant gradually decreases, and the light energy conversion rate and the number of photosynthetic products in the plant also decrease, which eventually leads to a decrease in the *SPAD* value in the plant.

The electrical signal is the change in membrane potential generated by tissues and cells in plants in response to external environmental stress [38]. It plays an important role in plant system communication [39–41]. The comparison between the physiological parameters of the plants and the electrical signal measurements has highlighted the possibility of using such electrical signals to detect the plant water status. In this experiment, we found that at the beginning of the drought stress, the soil relative water content in the DR treatment decreased most sharply on Day 2. On this day, the PTP and SD in the DR treatment showed significant differences compared with those in the CTRL treatment. Strawberry cells have a concentration difference between inner and outer cell membrane ions. As the cell membrane is semi-permeable and can actively take up extracellular ions, while intracellular ions are not easily leaked out, the cells have a certain resting potential at this time [42]. Under drought stress, the cell membrane senses the effective stimulus of drought stress, which leads to the opening of ion channels, K^+ spillover, temporary decrease in membrane resistance, and depolarization of membrane potential, and results in an action wave (AW). AW propagates in the protoplasmic continuous channel symplast of strawberry tissue, causing fluctuations in the electrical signal. The fluctuation of the electrical signal also causes a change in its SD [43]. However, as the stress level increases, this change becomes smaller, and the cells take up K^+ , gradually returning to a resting state to adapt to the new stress state. In the absence of timely water replenishment, the water in the plant and in the leaves decreases, and as the water deficit increases, both the tissue water content and the water potential of the leaves decrease. The reduction in water also reduced the electrical conductivity of the leaves, which caused a gradual decrease in cellular AV and a consequent decrease in PTP and SD until the plants died. The mean in the DR treatment did not show significant differences compared to that in the CTRL. This is because, although the mean is commonly used to quantify signal characteristics, it is an integral average of the plant electrical signal over the time axis, which describes only the statistical properties of the electrical signal over a period for a random signal [44]. Under external drought stress, the AW generated by changes in resting potential is a weak signal that is transmitted between cells and tissues. At the same time, as the plants adapt to drought stress and the AW disappears, the resting potential returns to stability, resulting in no significant difference in the mean of the electrical signal over time.

This experiment also revealed that strawberry seedlings' SCG and PSE changed more significantly during the early stages of drought stress. The power spectrum is the distribution of signal power with frequency, which characterizes the frequency properties of the signal and shows a degree of disorder in the time-series signal. The power spectrum of plant electrical signals essentially reflects the complexity of ion movement, potential distribution, and intercellular electrical coupling in the cell membrane [45]. On Day 6, the values of the SCG and PSE in the DR treatment were significantly higher than those of the CTRL. On this day, the relative soil humidity in the DR treatment was basically at its lowest value. As the drought stress on the strawberry seedlings gradually increased, the variation wave (VW) was produced in the stem, transmitting within plants. VW transmission often coincides with the transpiration rate of the plants. The production of VW requires a certain level of stress before it can be transmitted between plant tissues for a longer period [46]. VW transmission resulted in changes in F_v/F_m and *SPAD* parameters, thus reflecting

changes in transpiration in strawberry seedlings. Electrical signals are transmitted in plants from the stimulated cell or tissue to the cell or tissue where the physiological response occurs, mainly through living cells, especially the phloem, as there is less resistance to current flow in these cells [42,47,48]. This mechanism allows plants to respond quickly and accurately to environmental changes by generating electrical waves (AW and VW), which can be quantified in real-time. Therefore, electrical signals in plants can be used as early parameters of abiotic stress.

5. Conclusions

This study investigated the relationship between the electrical signals and physiological processes of strawberry seedlings under drought stress. Particularly, their chronological relationship is highlighted. The results indicate that electrical signals significantly differ between DR and CTRL treatment, and so do physiological parameters. However, the time of electrical signals presenting a significant difference precedes that of the physiological parameters. Therefore, the electrical signal can be used as an early indicator of drought stress conditions before physiological parameters change. This work provides a scientific basis for the water management of actual strawberry seedlings. It also provides a methodological and theoretical basis for the other study that analyzes the relationship between plant physiological parameters and electrical signals under other stress conditions (e.g., salt, high temperature, and cold and freezing stress pest disease).

It should be noted that this study selected three representative physiological parameters (chlorophyll fluorescence, maximal photochemical efficiency, and root vitality) to reflect plants' status under drought stress. However, there are other plant water-related parameters, such as relative water content in leaves and so on, that could also capture plants' status may present a significant difference between the control and drought treatment groups. Therefore, these parameters could be investigated in future studies.

Author Contributions: Planned the project, J.Q., J.Z. (Juan Zhou) and W.Y.; writing—original draft preparation, J.Z. (Juan Zhou), W.Y. and J.Q.; sampling and data collection, W.Y. and P.Z.; data analysis and result interpretation, B.D., J.Z. (Juan Zhou), W.Y. and T.D.; writing—review and editing, J.Q., J.Z. (Juan Zhou), J.Z. (Jianxi Zhu) and G.Z.; supervision and project administration, J.Q. All authors have read and agreed to the published version of the manuscript.

Funding: This research was supported by grants from the China Agriculture Research System (CARS-27). The funding organizations provided financial support to the research projects but were not involved in the design of the study, data collection, analysis of the data, or writing of the manuscript.

Institutional Review Board Statement: Not applicable.

Informed Consent Statement: Not applicable.

Data Availability Statement: The datasets generated during and/or analyzed during the current study are not publicly available due to [REASON(S) WHY DATA ARE NOT PUBLIC] but are available from the corresponding author on reasonable request.

Acknowledgments: We would like to thank Shuai Jiang, Yu Zhang, Xiangyang Yuan, Haoxuan Li, Bo Sun, Xiao Li, and Houze Guo for their extensive participation in the experiment.

Conflicts of Interest: The authors declare no conflict of interest.

Abbreviations

IPCC	the Intergovernmental Panel on Climate Change;
SOD	superoxide dismutase;
POD	peroxidase;
DR	drought treatment;
<i>d</i>	day;
CTRL	control treatment;

PTP	peak-to-peak value;
Mean	mean value;
SD	standard deviation;
SCG	Spectral of Central Gravity;
PSE	power spectrum entropy;
RV	root vitality;
Fv/Fm	maximal photochemical efficiency;
SPAD	the relative amount of chlorophyll;
AW	action wave;
VW	variation wave.

References

1. IPCC. *IPCC Launches Complete Synthesis Report. Contribution of Working Groups I, II and III to the Fifth Assessment Report of the Intergovernmental Panel on Climate Change*; IPCC: Geneva, Switzerland, 2015; 163p.
2. Janssen, T.; Fleischer, K.; Luyssaert, S.; Naudts, K.; Han, D. Drought resistance increases from the individual to the ecosystem level in highly diverse neotropical rainforest: A meta-analysis of leaf, tree and ecosystem responses to drought. *Biogeosciences* **2020**, *17*, 2621–2645. [[CrossRef](#)]
3. Sun, S.; Jung, E.; Gaviria, J.; Engelbrecht, B.M.J. Drought survival is positively associated with high turgor loss points in temperate perennial grassland species. *Funct. Ecol.* **2020**, *34*, 788–798. [[CrossRef](#)]
4. Seleiman, M.F.; Al-Suhaibani, N.; Ali, N.; Akmal, M.; Alotaibi, M.; Refay, Y.; Dindaroglu, T.; Abdul-Wajid, H.H.; Battaglia, M.L. Drought stress impacts on plants and different approaches to alleviate its adverse effects. *Plants* **2021**, *10*, 259. [[CrossRef](#)]
5. Dolfi, M.; Dini, C.; Morosi, S.; Comparini, D.; Masi, E.; Pandolfi, C.; Mancuso, S. Electrical signaling related to water stress acclimation. *Sens. Bio-Sens. Res.* **2021**, *32*, 100420. [[CrossRef](#)]
6. Chi, X.F.; Han, L. Research on plant adversity stresses. *Seed Sci. Technol.* **2019**, *37*, 122–124.
7. Luo, H.Y.; Jin, J.; Zhao, Q.L.; Deng, H.S.; Liao, C.F.; Fan, J.C.; Pu, T.L.; Han, X.Q. Research progress of drought stress on *Moringa oleifera* lam. *China Trop. Agric.* **2021**, *4*, 21–23, 72.
8. Zahedi, S.M.; Moharrami, F.; Sarikhani, S.; Padervand, M. Selenium and silica nanostructure-based recovery of strawberry plants subjected to drought stress. *Sci. Rep.* **2020**, *10*, 17672. [[CrossRef](#)]
9. Wang, D.; Sun, C.H. Effects of water stress on physiological characteristics of strawberry leaves. *Shandong Agric. Sci.* **2013**, *45*, 72–74. [[CrossRef](#)]
10. Klamkowski, K.; Treder, W. Response to drought stress of three strawberry cultivars grown under greenhouse conditions. *J. Fruit Ornament. Plant. Res.* **2008**, *16*, 179–188.
11. Ghaderi, N.; Siosemardeh, A. Response to drought stress of two strawberry cultivars (Cv. Kurdistan and Selva). *Hortic. Environ. Biotechnol.* **2011**, *52*, 6–12. [[CrossRef](#)]
12. Xue, X.P.; Liu, J. Effects of water stress on biochemical characteristics of apple seedlings. *North. Gard.* **2017**, *20*, 72–76.
13. Xiao, S.H.; Sun, H.B.; Zhang, W.Q.; Huang, F.F.; Gan, X.H.; Tang, C.B. Effect of drought stress on photosynthetic physiology of *Heritiera littoralis* seedlings. *J. For. Environ.* **2021**, *41*, 584–592. [[CrossRef](#)]
14. Shi, Y.J. The Effect of Drought Stress on Growth and Physiological Characteristics of Sassafras Tsumu Seedlings. Master's Thesis, Zhejiang A&F University, Hangzhou, China, 15 June 2016.
15. Zhang, Q.H.; Zeng, X.G.; Xiang, F.Y.; Han, Y.C.; Chen, F.Y.; Guo, C.; Han, Y.P.; Gu, Y.C. Effects on photosynthetic characteristics of strawberry seedlings under drought stress. *Hubei Agric. Sci.* **2016**, *55*, 6147–6150. [[CrossRef](#)]
16. Sanderson, J.B. Note on the electrical phenomena which accompany irritation of the leaf of *Dionaea muscipula*. *Nature* **1873**, *21*, 495–496. [[CrossRef](#)]
17. Brenner, E.D.; Stahlberg, R.; Mancuso, S.; Vivanco, J. Plant Neurobiology: An Integrated View of Plant Signaling. *Trends Plant Sci.* **2006**, *11*, 413–419. [[CrossRef](#)] [[PubMed](#)]
18. Schroeder, J.I.; Hedrich, R. Involvement of ion channels and active transport in osmoregulation and signaling of higher plant cells. *Trends Biochem. Sci.* **1989**, *14*, 187–192. [[CrossRef](#)]
19. García-Servín, M.Á.; Mendoza-Sánchez, M.; Contreras-Medina, L.M. Electrical signals as an option of communication with plants: A review. *Theor. Exp. Plant Physiol.* **2021**, *33*, 125–139. [[CrossRef](#)]
20. Datta, P.; Palit, P. Relationship between environmental factors and diurnal variation of bioelectric potentials of an intact jute plant. *Curr. Sci.* **2004**, *87*, 680–683.
21. Chatterjee, S.K.; Ghosh, S.; Das, S.; Manzella, V.; Vitaletti, A.; Masi, E.; Santopolo, L.; Mancuso, S.; Maharatna, K. Forward and inverse modelling approaches for prediction of light stimulus from electrophysiological response in plants. *Measurement* **2014**, *53*, 101–116. [[CrossRef](#)]
22. Wang, X.L.; Tian, L.G.; Li, M.; Li, Y.S. Analysis of the variation of electrical signals with illumination in the swallow palm. *Jiangsu Agric. Sci.* **2016**, *44*, 64–66, 141. [[CrossRef](#)]
23. Fromm, J.; Lautner, S. Electrical signals and their physiological significance in plants. *Plant Cell Environ.* **2007**, *30*, 249–257. [[CrossRef](#)] [[PubMed](#)]

24. Wang, Z.Y.; Fan, L.F.; Wang, Y.Q.; Li, J.H.; Zhou, Q.; Huang, L.; Wang, Z.Y. Selection of recording pattern of plant surface electrical signal based on analysis of electrical characteristics. *Trans. Chin. Soc. Agric. Eng.* **2018**, *34*, 137–143. [[CrossRef](#)]
25. Gao, X.; Xi, G.; Liu, K.; Liu, Q. The study of de-noising method about plant electrical signal based on wavelet. *J. Xi'an Univ. Technol.* **2013**, *29*, 92–97. [[CrossRef](#)]
26. Verma, N.; Verma, A.K. Performance analysis of wavelet thresholding methods in denoising of audio signals of some Indian musical instruments. *Int. J. Eng. Sci. Technol.* **2012**, *4*, 6.
27. Valencia, D.; Orejuela, D.; Salazar, J.; Valencia, J. Comparison analysis between rigrsure, sqtwolog, heursure and minimaxi techniques using hard and soft thresholding methods. In Proceedings of the 2016 XXI IEEE Symposium on Signal Processing, Images and Artificial Vision (STSIVA), Bucaramanga, Colombia, 31 August–2 September 2016; pp. 1–5.
28. Clemensson-Lindell, A. Triphenyltetrazolium chloride as an indicator of fine-root vitality and environmental stress in coniferous forest stands: Applications and limitations. *Plant Soil* **1994**, *159*, 297–300. [[CrossRef](#)]
29. Yu, X.L.; Zhang, J.B.; Wang, J. Relation between scalp potential and heart rate variability based on power spectral analysis. *J. Xi'an Jiaotong Univ.* **2007**, *41*, 991–994. [[CrossRef](#)]
30. Liu, Q.; Zhihui, L.I.; Jiyu, W.U. Research progress on leaf anatomical structures of plants under drought stress. *Agric. Sci. Technol.* **2016**, *17*, 4–7, 14. [[CrossRef](#)]
31. Nasir, M.W.; Toth, Z. Effect of drought stress on potato production: A review. *Agronomy* **2022**, *12*, 635. [[CrossRef](#)]
32. Šebelík, V.; Kuznetsova, V.; Lokstein, H.; Polívka, T. Transient absorption of chlorophylls and carotenoids after two-photon excitation of LHCII. *J. Phys. Chem. Lett.* **2021**, *12*, 3176–3181. [[CrossRef](#)]
33. Lunch, C.K.; LaFountain, A.M.; Thomas, S.; Frank, H.A.; Lewis, L.A.; Cardon, Z.G. The xanthophyll cycle and NPQ in diverse desert and aquatic green algae. *Photosynth. Res.* **2013**, *115*, 139–151. [[CrossRef](#)]
34. Zhang, K.; Chen, B.-H.; Hao, Y.; Yang, R.; Wang, Y.-A. Effects of short-term heat stress on PSII and subsequent recovery for senescent leaves of *Vitis vinifera* L. Cv. red globe. *J. Integr. Agric.* **2018**, *17*, 2683–2693. [[CrossRef](#)]
35. Hussain, M.I.; El-Keblawy, A.; Tsombou, F.M. Leaf age, canopy position, and habitat affect the carbon isotope discrimination and water-use efficiency in three C3 leguminous prosopis species from a hyper-arid climate. *Plants* **2019**, *8*, 402. [[CrossRef](#)] [[PubMed](#)]
36. Agrawal, D.; Jajoo, A. Study of high temperature stress induced damage and recovery in photosystem II (PSII) and photosystem I (PSI) in spinach leaves (*Spinacia oleracea*). *J. Plant Biochem. Biotechnol.* **2021**, *30*, 532–544. [[CrossRef](#)]
37. Ueki, K.; Iwamori, H. Geochemical differentiation processes for arc magma of the sengan volcanic cluster, northeastern Japan, constrained from principal component analysis. *Lithos* **2017**, *290–291*, 60–75. [[CrossRef](#)]
38. Xie, J.; Wu, Y.; Xing, D.; Li, Z.; Chen, T.; Duan, R.; Zhu, X. A comparative study on the circadian rhythm of the electrical signals of *Broussonetia papyrifera* and *Morus alba*. *Plant Signal. Behav.* **2021**, *16*, 1950899. [[CrossRef](#)]
39. Debono, M.W. Dynamic protoneural networks in plants. *Plant Signal. Behav. Dyn. Protoneural Netw. Plants* **2019**, *8*, e24207. [[CrossRef](#)]
40. Szechyńska-Hebda, M.; Maria, L.; Witoń, D.; Yosef, F.; Ron, M.; Karpiński, S.M. Aboveground plant-to-plant electrical signaling mediates network acquired acclimation. *Plant Cell* **2022**. [[CrossRef](#)]
41. Van, B.A.J.E.; Furch, A.; Torsten, W.; Buxa, S.V.; Rita, M.; Hafke, J.B. Spread the news: Systemic dissemination and local impact of Ca²⁺ signals along the phloem pathway. *J. Exp. Bot.* **2014**, *65*, 1761–1787. [[CrossRef](#)]
42. Gallé, A.; Lautner, S.; Flexas, J.; Fromm, J. Environmental stimuli and physiological responses: The current view on electrical signalling. *Environ. Exp. Bot.* **2015**, *114*, 15–21. [[CrossRef](#)]
43. Tracey, C.; Ingo, D.; Erwan, M. The role of potassium channels in arabidopsis thaliana long distance electrical signalling: AKT2 modulates tissue excitability while GORK shapes action potentials. *Int. J. Mol. Sci.* **2018**, *19*, 926. [[CrossRef](#)]
44. Lu, J.X. Research on relationship between environmental factors and features of electrical signals in plants. *Nanjing Agric. Univ.* **2012**. [[CrossRef](#)]
45. Zhang, C.; Wu, Y.; Su, Y.; Xing, D.; Dai, Y.; Wu, Y.; Fang, L. A Plant's electrical parameters indicate its physiological state: A study of intracellular water metabolism. *Plants* **2020**, *9*, 1256. [[CrossRef](#)] [[PubMed](#)]
46. Comparini, D.; Masi, E.; Pandolfi, C.; Sabbatini, L.; Dolfi, M.; Morosi, S.; Mancuso, S. Stem electrical properties associated with water stress conditions in olive tree. *Agric. Water Manag.* **2020**, *234*, 106109. [[CrossRef](#)]
47. Sukhov, V.; Sukhova, E.; Vodeneev, V. Long-distance electrical signals as a link between the local action of stressors and the systemic physiological responses in higher plants. *Prog. Biophys. Mol. Biol.* **2019**, *146*, 63–84. [[CrossRef](#)]
48. Ben Hamed, K.; Zorrig, W.; Hamzaoui, A.H. Electrical impedance spectroscopy: A tool to investigate the responses of one halophyte to different growth and stress conditions. *Comput. Electron. Agric.* **2016**, *123*, 376–383. [[CrossRef](#)]